Spring 2017

Epigenetic regulation of crx and nrl binding to regulatory elements in the genomes of human retinal neurons

Courtney B. Stout
James Madison University

Epigenetic Regulation of CRX and NRL Binding to Regulatory Elements in the Genome of Human Retinal Neurons

An Honors College Project Presented to

the Faculty of the Undergraduate

College of Science and Mathematics

James Madison University

by Courtney Brooke Stout

April 11, 2016

Accepted by the faculty of the Department of Biology, James Madison University, in partial fulfillment of the requirements for the Honors College.

FACULTY COMMITTEE:

Project Advisor: Raymond Enke, Ph.D.
Professor, Biology

Reader: Christopher Berndsen, Ph.D.
Professor, Chemistry

Reader: Jonathan Monroe, Ph.D.
Professor, Biology

HONORS COLLEGE APPROVAL:

Bradley R. Newcomer, Ph.D.,
Dean, Honors College

PUBLIC PRESENTATION

This work is accepted for presentation, in part or in full, at University of Maryland Baltimore County 19th Annual Undergraduate Symposium in the Chemical and Biological Sciences on 10/21/16.

Table of Contents

List of Figures and Tables

Figures

Tables

INTRODUCTION

Sight, as interpreted by our visual system, is our most important sense and is critical for deciphering our surrounding environment. Vision is achieved through the remarkable organization of diverse ocular cell types and tissues (1). The retina is a layered neuronal tissue lining the back of the eye containing rod and cone photoreceptors which convert light into an electrochemical signal to make vision possible (Figure 1A).

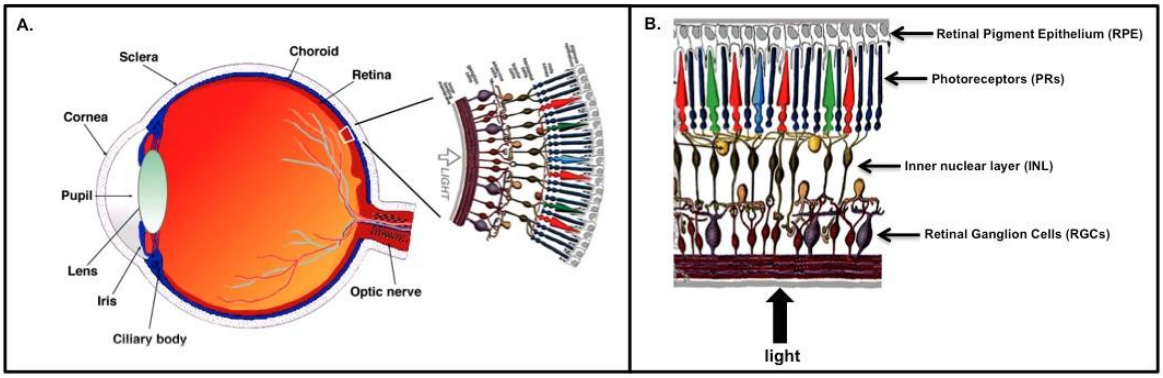

Figure 1. Anatomy of the eye (A) and layers of the retina (B). The vertebrate retina contains three layers of nerve cells, the outermost layer containing rod and cone photoreceptors, an inter neuronal layer containing bipolar, horizontal, and amacrine cells, and the innermost ganglion cell layer (1).

Visual impairment is a significant public health problem, particularly among the aging population. With the increasing median age of our national population, the number of individuals in the Unites States over 40 experiencing vision loss is expected to rise to 7 million by 2030 and 13 million by 2050 (2). Humans have limited ability to regenerate neurons, therefore vision loss associated with retinal degeneration is permanent. Some diseases resulting in vision loss are present at birth, and are associated with genetic mutations in retinal genes. Retinitis pigmentosa (RP) is a genetic disease that begins primarily with rod photoreceptor degeneration in the

peripheral retina and eventually leads to secondary cone degeneration in the late stages of the disease (3). Leber congenital amaurosis (LCA) is one of the most severe retinal dystrophies, as it affects humans within the first year of life and has been linked to six genetic mutations. Several diseases affect the macula of the eye, a region rich in cone photoreceptors that is involved in high acuity color vision. A disease that affects the aging population is macular degeneration, which is one of the leading causes of blindness in the U.S. Age-related macular degeneration is characterized by accumulation of lipid and protein-containing deposits called drusen that build up and cause damage to the cones of the macula region due to fluid leakage behind the fovea (3). Thus, studying the retina has significant public health impacts.

The vertebrate retina collectively contains three layers of nerve cells and two layers of synapses. The outermost layer contains rod and cone photoreceptors while the inner nuclear layer contains bipolar, horizontal, and amacrine cells. Lastly, the innermost ganglion cell layer contains the ganglion cell bodies and displaced amacrine cells. Just behind the outermost photoreceptor layer is the retinal pigment epithelium (RPE) (Figure 1B). RPE acts as a barrier between blood capillaries and retinal cells, is a support system for the retina, and works to recycle vital molecules for photoreceptor function. RPE is involved in the exchange of macromolecules, removal of shed membrane discs and retinoid recycling (1).

The fovea centralis is the spot in the center of the retina responsible for the highest acuity vision as it contains cone photoreceptors concentrated at maximal density. The 3 mm region around the fovea is known as the central retina, and the portion surrounding the central retina is known as the peripheral retina (Figure 2).

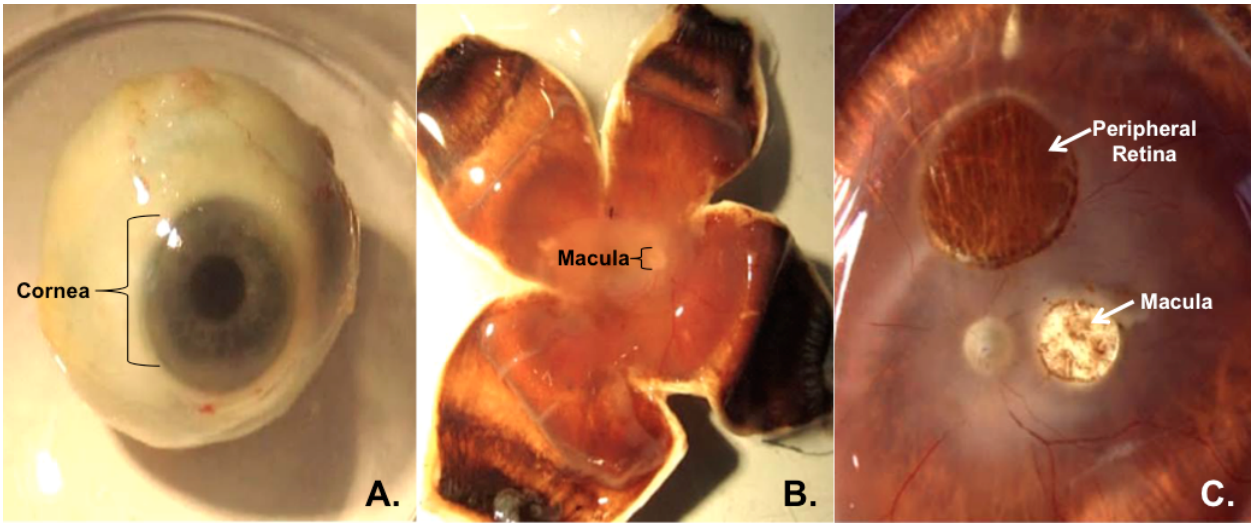

Figure 2. Tissue collection strategy of cornea, macula, and peripheral retina. The cornea is the translucent layer of tissue lying over the iris and pupil in the anterior portion of the eye in the area indicated by the bracket in (A). (B) shows a flat mount of the posterior portion of the eye used to collect tissues in the inner eye. In (C) biopsy punches of the peripheral retina and macula were collected as rod-rich and cone-rich retinal tissues respectively.

The peripheral retina is rich in rod photoreceptors and largely devoid of cone photoreceptors. In the center of the eye is the optic nerve responsible for transmitting the neuronal impulses from the retina to the brain. The optic nerve contains ganglion cell axons connecting the retina to the visual cortex of the brain, and is clustered close to blood vessels vascularizing the retina. The region of the retina through which the optic nerve passes is called the optic disk since this region lacks photoreceptors and therefore creates a blind spot in the retina. The ganglion cells lie in the innermost part of the retina, closer to the lens of the eye while the photoreceptors lie in the outermost portion of the retina, closer to the retinal pigment epithelium and choroid layers. The photoreceptors absorb photons of light and convert a biochemical signal to an electrochemical signal that stimulates the neurons of the retina.

Cone photoreceptors are conical shaped structures located mostly in the foveal region and are involved in high acuity color vision. Cones contain the visual pigments called cone opsins that are sensitive to long wavelengths of light between 420 nm and 650 nm. Most humans have trichromatic vision due to the presence of long wavelength-cones sensitive to red light, middle wavelength-cones sensitive to green light, and short wavelength-cones sensitive to blue light. Rods contain the visual pigment rhodopsin and are sensitive to shorter wavelengths of light (maximally sensitive at 496 nm of light) and are thus involved in low light or achromatic vision (1).

There are various groups of genes implicated in the phototransduction cascade that occurs in photoreceptors. Rhodopsin (*RHO*) is the is a transmembrane G-Protein coupled receptor (GPCR) expressed only in rod photoreceptors that contains a chromophore to absorb photons of light (4). The opsin cone pigments include the long-wave sensitive, medium-wave sensitive, and short-wave sensitive pigments known as *OPN1LW, OPN1MW*, and *OPN1SW.* The opsin cone pigment proteins OPN1LW, OPN1MW, and OPN1SW, are transmembrane GPCRs expressed exclusively in red, green, and blue cones respectively (5, 6) . Once light has been absorbed by the chromophores within photoreceptors, the GPCRs of rhodopsin or the cone opsin undergo conformation change and subsequently activate the heterotrimeric guanine nucleotide-binding proteins (G-proteins). Rod and cone-specific alpha subunits of the G-protein complex are coded for by *GNAT1* and *GNAT2* respectively (7, 8). Activation of the G-protein complex next results in activation of the phosphodiesterase 6 complex during the cascade. The PDE6 beta subunit in rods is coded for by the rod-specific gene *PDE6B,* while the cone-specific beta subunit is coded for by *PDE6C* (9). Activation of

phosphodiesterase causes hydrolysis of cyclic guanosine monophosphate (cGMP) and closure of cGMP-gated cation channels, thus resulting in hyperpolarization of the photoreceptor. Hyperpolarization decreases the amount of glutamate in the synaptic terminal resulting in release of the electric signal that can be processed by the postsynaptic neuron (10).

Complex transcription factor networks including the Cone-Rod Homeobox (CRX) transcription factor regulate phototransduction genes. CRX mutant analysis in mice has revealed the importance of the transcription factor in visual function (11). CRX knockout mice have dysfunctional photoreceptors that fail to develop normal outer segments, and thus this phenotype is accompanied by reduced expression of photoreceptor-specific genes including Rhodopsin (12). Deletion analysis paired with DNA binding assays revealed vital regulatory regions within CRX. A complete DNA binding domain is vital for the ability of CRX to bind DNA. Additionally, the OTX tail and WSP domain within CRX were determined to be necessary for transactivation activity of the transcription factor (11).

Mutations in the human CRX gene are associated with blinding diseases of the retina such as Leber congenital amaurosis, cone-rod dystrophy, and retinitis pigmentosa (13). CRX binds to cis-regulatory elements (CREs) in the genomes of rod and cone photoreceptors. Genome-wide CRX binding regions (CBRs) have been characterized the mouse retina (14). CRX has been found to bind predominantly to CREs with a known 8 bp motif, however, non-canonical CRX motifs with high GC content were also observed indicating a sequence context-independent feature of CRX binding to CREs (14, 15).

Among the many genes regulated by CRX is the rod-specific transcription factor Neural Retina Leucine zipper (NRL). NRL is a leucine zipper transcription factor expressed exclusively in rod photoreceptors. Deletion of NRL in mice results in complete loss of rod function. An important mouse model used to study gene expression in the retina is the Nrl -/- mutant retina. Nrl -/- mice experience loss of rods replaced by S-cones (short wave blue cones) within their retinas (16). The Nrl -/- phenotype is associated with complete loss of rod function and super-normal cone function. However, the cones in Nrl -/- retina have short outer segments with abnormal disks. The function of NRL as a transcription factor is to direct rod cell development by activating transcription of rod-specific genes while inhibiting formation of S-cones via activation of the nuclear receptor subfamily 2, group E, member 3 transcription factor, also known as Nr2e3 (16). Over 300 genes have been associated as direct target genes of NRL, 22 of which are loci associated with human retinal diseases. Knockdown of 16 of these NRL target genes resulted in photoreceptor-cell death of abnormal rod photoreceptors. High enrichment of NRL binding sites overlapping with CRX binding sites suggests that CRX and NRL work together to control rod photoreceptor cell fate (17). Additionally, mutations in NRL are also associated with degenerative diseases of the retina such as dominant and recessive retinitis pigmentosa (13). A better understanding of the transcriptional networks controlled by CRX and NRL in photoreceptor development and maintenance will be critical for developing novel therapeutic and replacement strategies for blinding retinal neuropathies.

Transcriptional networks are known to be modulated by epigenetic modifications to the genome (18). Epigenetic modifications can be organized into two broad

classifications: histone tail modifications and genomic DNA methylation (19). Histone modifications are covalent, post-translational changes to the histone proteins around which DNA is wrapped to make up chromatin. Histone modifications include acetylation, methylation, phosphorylation, ubiquitination, and various other modifications that modulate gene expression by changing the chromatin structure or by altering accessibility of DNA to regulatory proteins (20). Epigenetic modifications to the chromatin can result in transcriptional repression or activation depending on the context and type of modification. DNA methylation and histone modifications work in combination to recruit protein complexes to regulate transcription (21). Recently, it has been suspected that there is cross talk between DNA methyltransferases and histone methyl transferases in regulating transcriptional activity (19).

DNA methylation is an epigenetic modification that involves addition of a methyl group to the fifth carbon position of a cytosine residue in a 5'-CpG-3' dinucleotide (CpG). DNA methylation is typically associated with a repressed transcriptional chromatin state and therefore is inversely correlated with gene expression when accumulated in 5' gene regulatory regions. Differentiation of the retina from neuronal precursors is a highly regulated process that involves coordinated control of gene expression during development (23). *De novo* DNA methylation in mammals primarily occurs during gametogenesis and embryogenesis (22). Thus, DNA methylation may play a role in control of gene expression during development of the retina. Several photoreceptor-specific genes have exhibited a cell-specific differential DNA methylation pattern inversely correlated with their expression level. Differential methylation patterns were observed in *rhodopsin* (*RHO*), *retinal binding protein 3* (*RBP3*) *cone opsin, short-*

wave-sensitive (*OPN1SW*), *cone opsin, middle-wave-sensitive* (*OPN1MW*), and *cone opsin, long-wave-sensitive* (*OPN1LW*), which suggests that DNA methylation is an important modification in controlling photoreceptor gene expression (23).

DNA methyltransferases (DNMTs) are the enzymes that catalyze the addition of a methyl group to cytosine residues. Establishment and maintenance of DNA methylation in the genomes of plants and vertebrates is essential for development (24). The role of Dnmt3a and Dnmt3b is to establish *de novo* methylation followed by subsequent maintenance of methylation imprints by Dnmt1 during DNA replication. Mutation of Dnmts in the vertebrate retina results in transcriptional dysregulation and retinal degeneration. These finding supports the importance of DNA methylation in modulating expression of photoreceptors in the retina (25).

A more recent discovery in epigenetics is the presence of an active demethylation pathway mediated by the oxidation of 5mC to 5-methylhydroxycytosine (5hmC). Hydroxymethylation of 5mC is catalyzed by the ten-eleven translocation (TET) family of enzymes. Active DNA demethylation triggered by the TET oxidation of 5mC to a 5hmC initiates a base excision repair mechanism removing a stretch of DNA including the epigenetically modified nucleotide(s) and replacing them with unmodified cytosines (26). Neuronal tissue demonstrates relatively high levels of the 5hmC epigenetic mark in vertebrate species indicating a potential role for active demethylation neuronal gene regulation (27).

DNA methylation plays an essential role in cell fate in the retina and has disease implications in the retina since methylation has been linked to regulation of neuronal cell death in the retina. Programmed cell death plays an important role in vertebrate eye

morphogenesis and occurs selectively in certain cell types. A directed cell death process that is regulated by epigenetic mechanisms such as DNA methylation and hydroxymethylation characterizes the loss of photoreceptors caused by degenerative diseases in the retina. Cell-specific increases in DNA methylation and hydroxymethylation in the retina of normally developing mice as well as in an RP-like degenerated mouse retina were observed through immunostaining (28). During normal development of the retina, characterized by apoptotic cell loss in the inner retina, increases in methylation and hydroxymethylation were detected. Similarly, increased methylation and hydroxymethylation was detected in early stages of photoreceptor degeneration (29). Since Dnmts are expressed in retinal progenitors as well as in mature retinal neurons, this suggests the importance of DNA methylation in establishing normal cell-specific methylation patterns to control differentiation in the retina. The detection of hydroxymethylation during retinal degeneration and development also suggests that there is likely a homeostatic balance in retinal neurons established by both methylation and demethylation (leads to formation of hydroxymethylation), and the process of retinal degeneration involves complex pathways of methylation and demethylation (28).

Previously, our lab has demonstrated that there is a tissue-specific pattern of DNA methylation in retina specific genes (Figures 4 and 6). Furthermore there is an inverse correlation between DNA methylation and mRNA expression. This inverse correlation between DNA methylation and mRNA expression was observed in a subset of genes analyzed, specifically in the rod-specific genes *RHO, NRL*, and *PDE6B*, as well as in the *CRX* gene expressed in both rods and cones. Additionally, cell type-

specific patterns of DNA methylation were also observed within rod and cone photoreceptors. Conserved regulatory regions controlling photoreceptor-specific genes in which low methylation was observed with a presence of CRX or both CRX and NRL binding sites supported the cell-specific pattern of methylation between rods and cones.

CRX binds to cis-regulatory elements in DNA and interacts with transcriptional co-activator protein complexes with histone acetyltransferase (HAT) activity (30). Transcription of rod and cone opsin genes requires binding of CRX followed by recruitment of HATs, acetylation of histone 3 (H3ac), and subsequent binding of other transcriptional activators such as NRL as well as RNA polymerase II. This sequence of events occurs in promoter and enhancer regions of both rod and cone opsin genes (30). These interactions mediate physical contact of the enhancer and promoter as well as other coding regions in each opsin locus forming an intrachromosomal loop that drives expression of photoreceptor-specific genes (31). It is currently not known however, what mediates differential recruitment and binding of CRX in rod and cone photoreceptors genomes. I hypothesized that observed patterns of differential DNA methylation on CRX binding sites modulates the ability of the transcription factor to bind cis-regulatory elements. This hypothesis predicts that DNA demethylation of regulatory elements precedes CRX binding and is therefore the initiating event in photoreceptor-specific gene expression. Bisulfite pyrosequencing analysis was used to examine tissue and cell-specific patterns of DNA methylation in photoreceptor-specific genes of the retina in murine and human samples. Additionally, the purified CRX protein was used to conduct in vitro binding assays to characterize how DNA methylation and hydroxymethylation modulate CRX binding in the genome of human retinal neurons.

METHODS

Tissue Collection and Bisulfite Conversion of DNA for PCR Amplification

Post-mortem human donor eyes collected from the National Disease Research Interchange were used to dissect out relevant tissues for quantification of DNA methylation in retina-specific genes. Corneas were removed first from the donor eyes and were placed on dry ice and ground into a powder. Retinal flat mounts were prepared by making 4 radial cuts into the remaining eye cup and taking a 3 mm biopsy punch of the macular retina (cone-rich tissue) and a 6 mm biopsy punch of the peripheral retina (rod-rich tissue). Tissue samples were placed in Qiagen RNeasy Lysis buffer and beta-mercaptoethanol to lyse the cells. Extracted DNA underwent bisulfite (BS) conversion using the Zymo EZ DNA MethylGold Kit. Unmethylated cytosine bases are converted to uracil during bisulfite conversion via attachment of a sulfite group to the cytosine and subsequent deamination and desulfonation to uracil. Methylated cytosines remain unchanged during conversion, and thus the amount of methylation in various retinal genes can be quantified through subsequent PCR amplification and pyrosequencing.

Either the forward or the reverse primer used in the polymerase chain reaction (PCR) were biotinylated, and thus one strand of the PCR amplicon became tagged with biotin to allow a specific strand to be marked for the sequencing reaction. BS PCR reactions were set up in 30 uL volumes using Sigma-Aldrich JumpStart Taq polymerase and gene-specific primers were used to amplify BS converted DNA from ocular samples (Table 2). DNA from peripheral retina, macular retina, and cornea were set up in

triplicate for each PCR reaction. PCR reactions were run at optimized annealing temperatures on a Bio-Rad C1000 Touch Thermal Cycler.

Bisulfite Pyrosequencing

PCR products were mixed with streptavidin-conjugated beads and a sequencing primer and a Qiagen Q24 Pyrosequencer was used to determine percent methylation at CpG dinucleotides in the BS PCR amplicons. Percent methylation between triplicates of each DNA sample was averaged, and methylation plots were visualized in Graph-Pad Prism. Statistical significance between macula and peripheral retina was determined by a one-tailed t-test with a p value threshold set at <0.05.

Expression of human CRX and NRL

Protein expression plasmids containing full-length and DNA binding domain (DBD) coding sequences for the human CRX and NRL proteins fused to epitopes for protein purification were purchased from Genscript. Constructs were transformed into BL21 DE3 *E. coli* competent cells and transformants were selected for on lysogeny broth plates containing either kanamycin for the full-length constructs or carbenicillin for the DBD constructs. Single colonies were selected from each plate to set up broth cultures for induction of protein expression with isopropyl β-D-1-thiogalactopyranoside (IPTG). Starter cultures containing 3 mL of LB and 2.5 uL of kanamycin (for full length constructs) or carbenicillin (for DBD constructs) were inoculated with a single colony from the each culture plate. Starter cultures were incubated in a shaking incubator at 37°C and 230 rpm for 12 hours. Small-scale expression cultures were set up using 2 mL of the starter cultures, 300 mL of LB, and 240 uL of the corresponding antibiotic. Small-scale expression cultures were incubated (at 37°C and 230 rpm) until the optical density

(OD) of the culture reached 0.5-0.6 as determined by spectrophotometry. The spectrophotometer was set at 600 nm with a 1 cm path length cell, and was blanked with LB prior to each OD reading. After reaching the desired OD, 60 uL 0.2 mM IPTG was added to each culture. Aliquots of expression cultures were taken out of each culture prior to induction; as well as 1.5 and 3 hours after induction. Post-induction time course experiments were conducted using polyacrylamide gel electrophoresis (PAGE) analysis.

Purification of human CRX and NRL

Small-scale purification using a nickel-column was performed using the batch cultures of protein lysates from the 3-hour post-induction time point. Bacterial cells were incubated in protein lysis buffer (50 mM sodium phosphate (pH 8), 300 mM NaCl, and 1 mM BME; 0.001 mM lysozyme) in a water bath at 37°C for 5 minutes to lyse the cells. Samples were sonicated for 60 seconds total at an amplitude of 40% using a 5 second on/off pulse, and the cycle was repeated twice. Lysates were then treated with a nuclease mixture, prepared from 2 µL of nuclease and 20 µL of 1 M $MgCl_2$, to help degrade viscous DNA from the lysates. Samples were centrifuged at 4°C and 15,557 x G for 30 minutes to pellet the insoluble materials. Aliquots of the supernatant as well as the pellet were saved for SDS-PAGE. The remaining supernatant was used for further purification with the nickel column.

To prepare the nickel beads for use in the column, 1 mL portions of nickel bead slurry were prepared by centrifuging at 750 rpm for 5 minutes. The supernatant of the bead slurry was discarded. The remaining protein supernatant was added to the pellet of beads. The protein-bead mixture was incubated at 4°C while shaking. To elute the

His-tagged proteins from the column containing the nickel beads, imidazole was used. Three concentrations of imidazole (10 mM, 40 mM, and 250 mM) diluted in lysate buffer were prepared in 50 mL volumes. The pH of the imidazole solutions in lysis buffer was brought to 8.

Approximately 10 mL portions of the prepared protein-bead mixtures of each sample were allowed to slowly flow through the nickel column. The protein-bead mixture tubes were rinsed with lysis buffer to ensure no residue was left in the tube. The column was then washed with 5 mL of lysis buffer. To elute each protein of interest from the column, 5 mL washes of 10 mM imidazole, 40 mM imidazole, and 250 mM imidazole were used. Each fraction was collected and saved after flowing through the column for SDS-PAGE. The nickel column was not allowed to dry out, and approximately 1 mL of each solution was always left in the column to prevent drying.

Bio-Rad Mini-PROTEAN TGX Stain Free Pre-cast gels were used with a 1X tris/glycine/sodium dodecyl sulfate buffer system. Bio-Rad Precision Plus Unstained Protein Standards (250 kD) were run on the gel as the marker. Protein samples were mixed with 2X Laemmli Sample Buffer. Protein samples were prepared to run on the gel by vortexing briefly and boiling for 5 minutes.

Bioinformatics Analysis of CRX and NRL Binding Sites

CRX binding regions (CBRs) as well as NRL binding regions (NBRs) obtained from published murine chromatin immunoprecipitation sequencing data were mapped as custom Browser Extensible Data (BED) annotation tracks in the University of California Santa Cruz Genome Browser (genome.ucsc.edu). CBR data was obtained from Corbo et al., (2010), and NBR data was obtained from Hao et al., (2012). The

LiftOver tool in the UCSC Genome Browser was used to align the CBRs and NBRs from the July 2007 mouse NCBI37/mm9 genome assembly to the human February 2009 GRCh37/hg19 assembly. Aligned murine CBRs and NBRs to the human genome were added as custom tracks in the UCSC Genome Browser. Additionally, CRX binding motifs were added as a custom track using data obtained from the Motif Map database.

A Plasmid Editor (ApE) was used to annotate the *Rhodopsin* genomic sequence to determine relevant cytosine methylation sites for binding assays. The *Rhodopsin* DNA sequence was annotated with CBRS, NBRs, and CRX binding motifs in ApE using the custom tracks created in the hg19 assembly of the UCSC Genome Browser.

Synthesis of Epigenetically Labelled DNA Probes

Two primers were used to amplify regions of interest in the human *Rhodopsin* gene to create probes for in vitro binding assays. The F1/R1 primer was used to synthesize the 150 bp enhancer region (-6 kb upstream from exon 1) in *Rhodopsin* and the F2/R2 primer was used to synthesize a 129 bp enhancer region adjacent to the first exon of Rho. F1/R1 and F2/R2 refer to abbreviations used to identify the primers in Table 2. PCR reactions were set up in 30 uL volumes using Sigma-Aldrich REDTaq DNA Polymerase and human retinal pigment epithelium DNA. The different types of deoxynucleotides (dNTPs) were added separately to their respective PCR reaction to create epigenetically labeled probes. Normal dNTPs, 5mC dNTPs, a 1:1 mix of normal dNTPs with 5mCs, 5hmCs, and a 1:1 mix of normal dNTPs with 5hmC dNTPs were used to create each EMSA probe using the respective primer. Additionally, a no dNTP control was set up. PCR reactions were run at optimized annealing temperatures on a Bio-Rad C1000 Touch Thermal Cycler. The 5mC-sensitive and 5hmC-sensitive

restriction enzymes HaeIII and Cac8I were used to verify the synthesis of epigenetically labeled probes. Digested probe fragments were run on a 1.2% agarose gel stained with GelRed.

In Vitro Binding Assay (EMSA)

In vitro binding assays were carried out using 15 uL of the F1/R1 or F2/R2 EMSA probe PCR product, mixed with 50 mM EDTA to help minimize nuclease activity of the protein, and 30 uL of the CRX DBD purified protein. Samples were incubated for 30 minutes at room temperature. Samples not mixed with protein were prepared using 15 uL of the F1/R1 or F2/R2 EMSA probe PCR products with 2 uL of EDTA and 30 uL of 10 mM MOPS; 100 mM NaCl buffer (3-(N-morpholino)propanesulfonic acid). Samples were run on a 2.5% agarose gel containing GelRed. The gel was run at 50 V for approximately 3.5 to 4 hours.

RESULTS

Cell and Tissue Specific Patterns of DNA Methylation in Mouse Models

The initial pattern of tissue and cell-specific DNA methylation in genes of the retina was examined in the mouse model. Primers designed to amplify conserved promoter CRX binding regions (CBRs) were used to conduct bisulfite pyrosequencing analysis to study the pattern of methylation in genes specific to the retina (Figure 3).

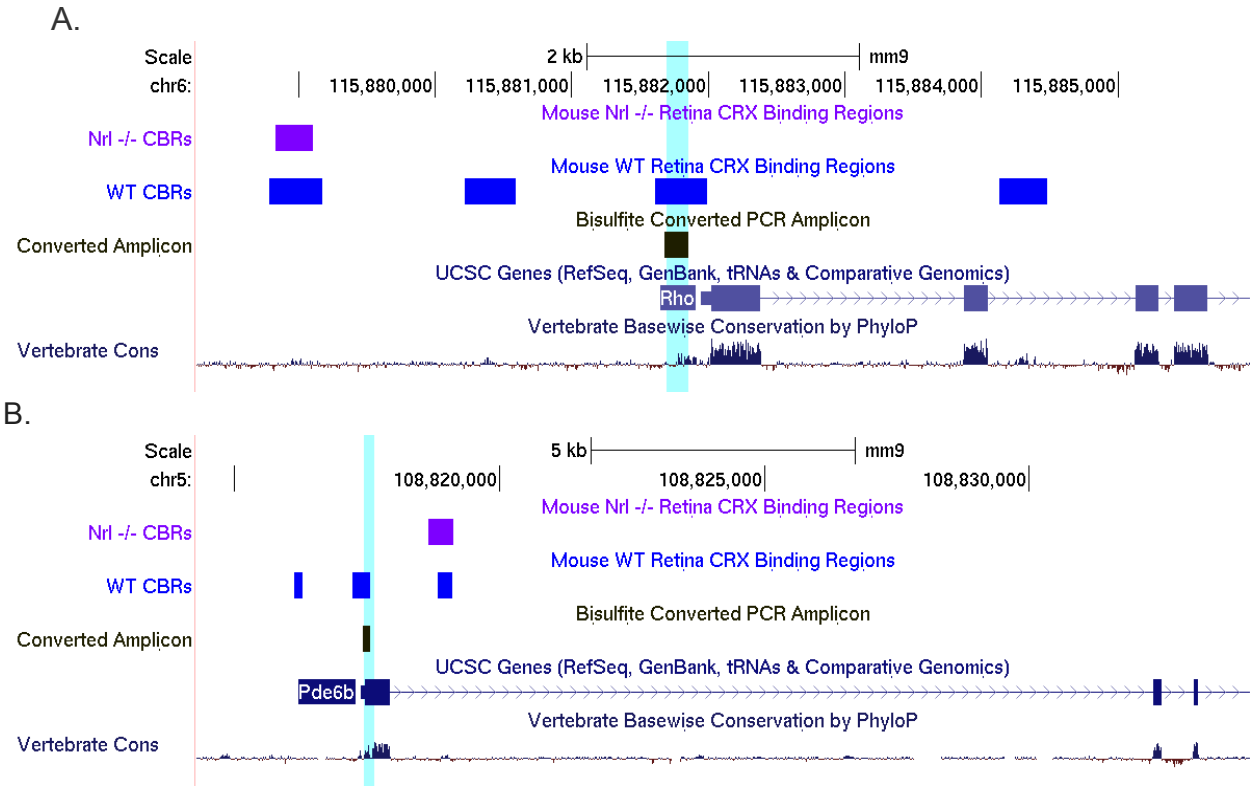

Figure 3. Genome Browser View of the 5' Regions of Rhodopsin and PDE6B in the mouse genome. The purple Nrl -/- CBRs track shows CRX binding regions in the nearly all cone Nrl -/- retina. The dark blue WT CBR alignments track shows CRX binding regions. The PCR amplicon regions analyzed by bisulfite pyrosequencing are represented in black. The relative DNA conservation between 100 species of vertebrates is represented in the bottom track. Light blue highlighted regions represent areas where CRX is predicted to be able to bind due to the presence of highly conserved CRX binding regions.

Bisulfite pyrosequencing revealed a tissue and cell-specific pattern of DNA methylation in genes specific for subunits of photoreceptors in the retina (Figure 4). Samples of Nrl mutant retina (Nrl -/-) composed of nearly all cones and CRX mutant (CRX -) retina composed of dysfunctional photoreceptors lacking mature outer segments accompanied by reduced expression of photoreceptor-specific genes were compared to wild type retina and wild type brain. Wild type retina contains functional rod and cone photoreceptors, while wild type brain lacks photoreceptors.

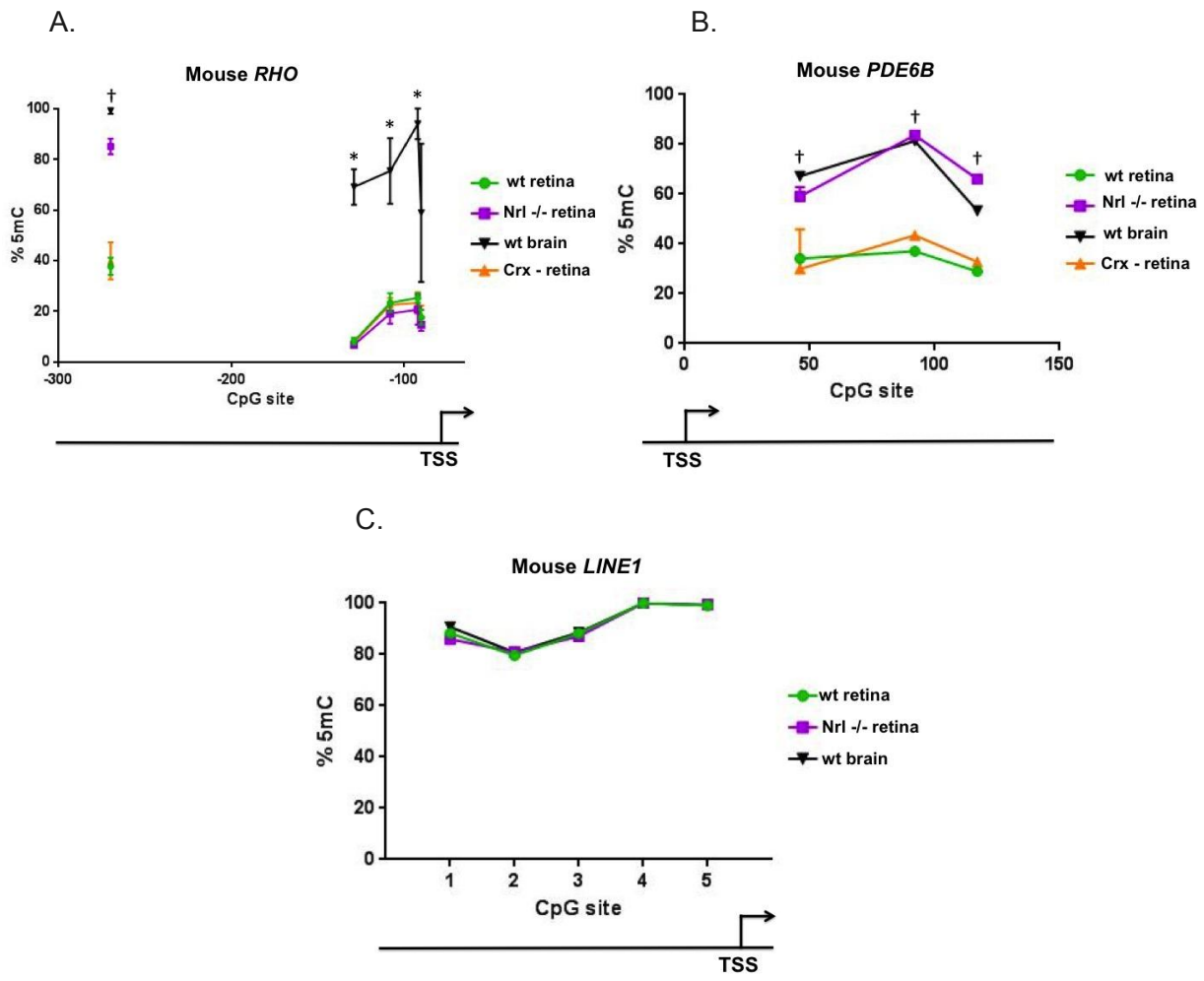

Figure 4. Bisulfite pyrosequencing analysis of Mouse DNA methylation at CpG sites relative to the transcriptional start site of (A) Rhodopsin, a rod photoreceptor gene, (B) Phosphodiesterase-6b, another rod-specific photoreceptor gene, and (C) LINE1 retrotransposon repeats. Error bars represent standard error of three replicates of each sample. Statistical significance of both Nrl -/- retina and wt brain determined by a one-tailed t-test with a $p<0.05$ are denoted by (†). Statistical significance of only wt brain determined by a one-tailed t-test with a $p<0.05$ is denoted by (*).

In the proximal promoter sequence of the mouse rod-specific *RHO* gene, wt brain had significantly higher methylation compared to wt retina, Nrl -/- and Crx - retina. At the upstream *RHO* enhancer site analyzed using a separate PCR primer, wt brain as well as Nrl -/- retina had significantly more methylation than wt retina and Crx - retina. This pattern suggests that wt brain, devoid of photoreceptors has higher methylation than

retinal samples containing some form of photoreceptors. The observation that Nrl -/- retina did not have significantly higher methylation at all sites analyzed in the Rhodopsin gene is not entirely consistent with the predicted pattern that a sample of retina composed of nearly all cones would have high methylation in a rod-specific photoreceptor gene. However, Phosphodiesterase-6b (*PDE6B*), another rod-specific photoreceptor gene, did show a more consistent pattern of cell-specific DNA methylation. At each CpG site analyzed in the *PDE6B* gene, both wt brain and Nrl -/- retina had significantly more methylation than wt retina and Crx - retina. Thus, the *PDE6B* gene shows both a tissue and cell-specific pattern of methylation. As a positive control, *LINE1*, a constitutively methylated retrotransposon repeat element, showed no difference in methylation among samples since this gene is highly methylated at all times (Figure 4).

Cell and Tissue Specific Patterns of DNA Methylation in Human Models

Observations of tissue and cell-specific patterns of DNA methylation in the mouse model prompted further investigation in primary human retinal neurons. A similar setup to the mouse experiment using various photoreceptor enriched tissues in human donor eyes was used to conduct bisulfite pyrosequencing analysis in humans. Cornea was collected as a non-retinal control tissue from human donor eyes (Figure 1A). After creating a retinal flat mount, 6 mm biopsy punches of peripheral retina as well as 3 mm biopsy punches of macula were collected (Figure 1B and 1C). Peripheral retina served as a rod-enriched tissue while macula served as a cone-enriched sample (Figure 1C).

Information regarding post-mortem human donor eyes used for tissue collection of cornea, peripheral retina, and macula is recorded in Table 1. Primers designed for both mouse and human methylation analysis are listed in Table 2.

Table 1. Human donor eye patient information.

Sample ID	Age	Race	Sex	Death:enucleation (hours)	Death:delivery (hours)
Eye# 8670	Unknown	Unknown	Unknown	Unknown	Unknown
Eye #7	75	caucasian	M	7.2	27
Eye #8	78	caucasian	M	5.1	45.58
Eye #9	82	caucasian	M	6.75	35.9

Table 2. Oligonucleotides used for bisulfite PCR, pyrosequencing and analysis and EMSA probe synthesis.

Primer Name	Sequence (5'-3')	Region Analyzed	Amplicon Size (bp)	Annealing temp (˚C)	Application
hLINE1F	proprietary (Qiagen product #970042)	Human LINE1 retrotransposon promoters	146	50	BS PCR
hLINE1R-BIO	proprietary (Qiagen product #970042)				BS PCR
hLINE1-seq	proprietary (Qiagen product #970042)				pyrosequencing
hPax6-F1	TAGTTATAGGTYGGGTTAAGGAAGGTTAAA	Human PAX6 promoter	248	54-58	BS PCR
hPax6-R1-bio	AACCTACCCCAAAATTTAAATATCAA				BS PCR
hPax6-seq1	ATTAGTYGGYGTAGAGTTGTGTTTA				pyrosequencing
JS_BS_hRho_F3	TTGAGTTGGGATTTTGGGATAGATAAG	Human RHO promoter	241	54-58	BS PCR
JS_BS_hRho_R3_biotin	TATAAAATAACCTCCCCCTCCT				BS PCR
JS_BS_hRho_S3	TTTGGTTTTTTTTAGAAGTTAATTA				pyrosequencing
JS_hRho_F4	AGGGGTTTGTAAATAAATGTTTAATGA	Human RHO upstream promoter	258	54-56	BS PCR
JS_hRho_R4-Bio	ACTTTCTAATTTATTCTCCCAATCTCT				BS PCR

JS_hRho-seq4-2	ATTGGATGATTTTAGAGGT				pyrosequencing
hPde6b-F1	TGGGAAGTTTTAGGGTTTGAGG	Human PDE6B Promoter	120	54-58	BS PCR
hPde6b-R1-bio	AAAACCCTATCATCAACAAAATCTTTCTTA				BS PCR
hPde6b-seq1	TTTAGGGTTTGAGGAGA				pyrosequencing
hRER-F2-Bio	GTGGGTTAGTTTTGATTTAAGGTAT	Human RHO Enhancer	284	54-62	BS PCR
hRER-R2	CCCAAAATTCCCAAATCTATCTACTCAA				BS PCR
hRER-seq2-1	ACAAAACCAATAAAATAAAACCTCT				pyrosequencing
EMSA-En-F1-BIO	AAGAAAGCCAAGGAAGAGGAGGAG	Human RHO -5 kb enhancer	150	54-64	probe for EMSA
EMSA-En-R1	TTTGCCTTTGCCTCGGTGGATTAG				probe for EMSA
EMSA-RER-F2-BIO	ACCCTCACCTTAACCTCATTAGCG	Human RHO RER	129	54-64	probe for EMSA
EMSA-RER-R2	TGGTGTTGGGTCTAACAGCGTTTG				probe for EMSA
VO_mPde6b_F1	GTATTTGGGGGTGGAGAAAG	Mouse PDE6B Promoter	152	58	BS PCR
VO_mPde6b_R1_bio	ACAAACCCCTACCACATTTTCAAA				BS PCR
VO_mPde6b_S1	GGGGGTGGAGAAAGT				pyrosequencing
REmL1_F1	TTTTTTGGGGTTAGGATTTGGGGTATAAG	Mouse LINE1 retrotransposon promoters	211	54	BS PCR
REmL1_R1_Bio	AACCTACTTCCCTATATACTACAATCT				BS PCR
REmL1_seq1	GATTTGGGGTATAAGTTTTT				pyrosequencing
KTmRho-F1	AGGGAGAGAAGGTTATTTTATAAGG	Mouse RHO Promoter	177	58	BS PCR
KTmRho-R1	AACACATAAAAATTAAAACCCTCTATAC				BS PCR
KTmRho-S1	GGGGTTAGTGTTTGGA				pyrosequencing
VO_m_Rho_F1	AGAGGATTTTGGGGTAGATAAG	Mouse RHO Promoter	169	58	BS PCR
VO_m_Rho_R1_bio	TCCCTAAACCAAAAACTAATTCAACA				BS PCR
VO_m_Rho__S1	ATTTTTTTTTTTTTTTATTTAAGGG				pyrosequencing
VO_m_Rho_S2	ATTTTGGTTTTTTTGTAAGTTAAT				pyrosequencing
REmRho(-270)-F1	TGAGTTTAGGAGGAGATATTGTTAAT	Mouse RHO Promoter	125	58	BS PCR
REmRho(-270)-R1-bio	CCCCAAAATCCTCTAAAAATTCCT				BS PCR
REmRho(-270)-seq1	AGTGAATTTAGGGTTTAAAG				pyrosequencing
REmRho(up RER)-F1	GGGGTTGTTTTTGTTATTTAAGTGAGAGAG	Mouse RHO Enhancer	219	58	BS PCR
REmRho(up RER)-R1-Bio	CCTCAACAACCTCTACAACCAACTTATA				BS PCR
REmRho(up RER)-seq1	AGAGTTTAGGAGATGG				pyrosequencing

REmRho(down RER)-F1	AGGAAGGGGGTTGTTTTTTTAA	Mouse RHO Enhancer	182	58	BS PCR
REmRho(down RER)-R1-Bio	CTATACCCCTTACCACATAAATATCC				BS PCR
REmRho(downs RER)-seq1	GGGTTGTTTTTTTAAGTAAATAT				pyrosequencing

Bioinformatics analysis was used to determine regions of interest for studying DNA methylation patterns in the human genome where CRX may be able to bind. In addition to mapping the CRX binding regions (CBRs) obtained from previous mouse ChIP-seq data, CRX binding motifs lifted over from the mouse genome to the human genome were mapped to determine areas in which CRX is likely to bind. Conserved regions of the human genome containing CRX binding regions with CRX motifs were analyzed by bisulfite pyrosequencing analysis to investigate methylation patterns in retina-specific genes (Figure 5).

A similar pattern of tissue and cell-specific DNA methylation observed in photoreceptor genes of the retina in mice was also observed in the human study. Both human rod-specific genes *RHO* and *PDE6B* demonstrated significantly higher methylation in cone-enriched macula as well as non-retinal cornea samples compared to rod-rich peripheral retina (Figure 6). *LINE1*, a constitutively methylated retrotransposon repeat element, as well as *PAX6*, an unmethylated eye field gene expressed constitutively in the retina, showed no significant difference in methylation among cornea, macula, and peripheral retina (Figure 6).

A.

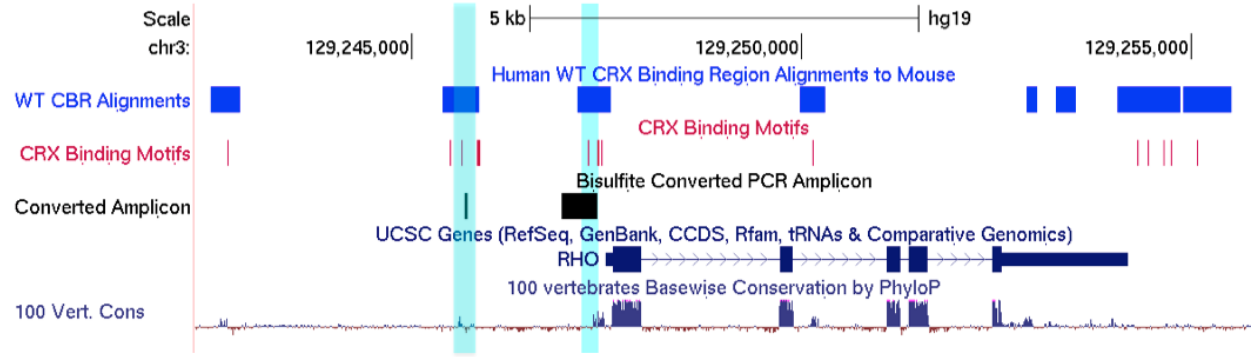

B.

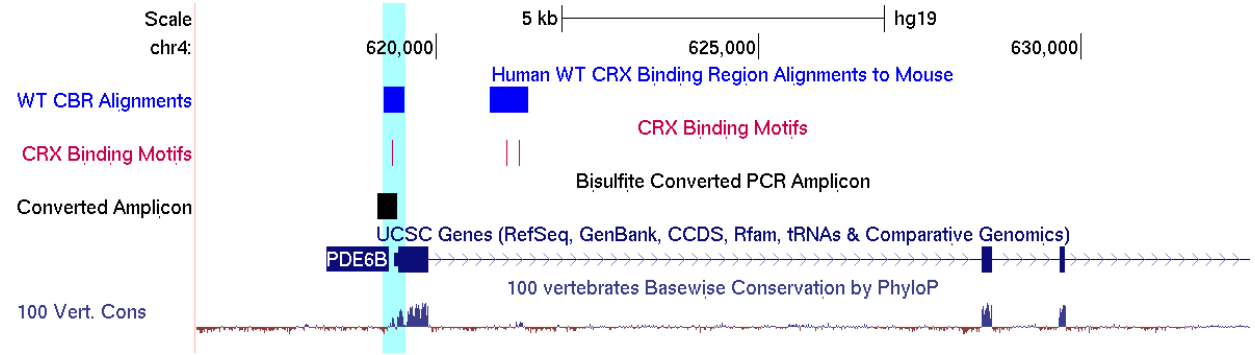

Figure 5. Genome Browser View of the 5' Regions of Rhodopsin and PDE6B. The blue WT CBR alignments track shows murine CRX binding region data that has been aligned to the human genome. CRX binding motifs are represented in pink, along with the PCR amplicon regions analyzed by bisulfite pyrosequencing. The relative DNA conservation between 100 species of vertebrates is represented in the bottom track. Blue highlighted regions represent areas where CRX is predicted to be able to bind due to the presence of highly conserved CRX binding regions with binding motifs.

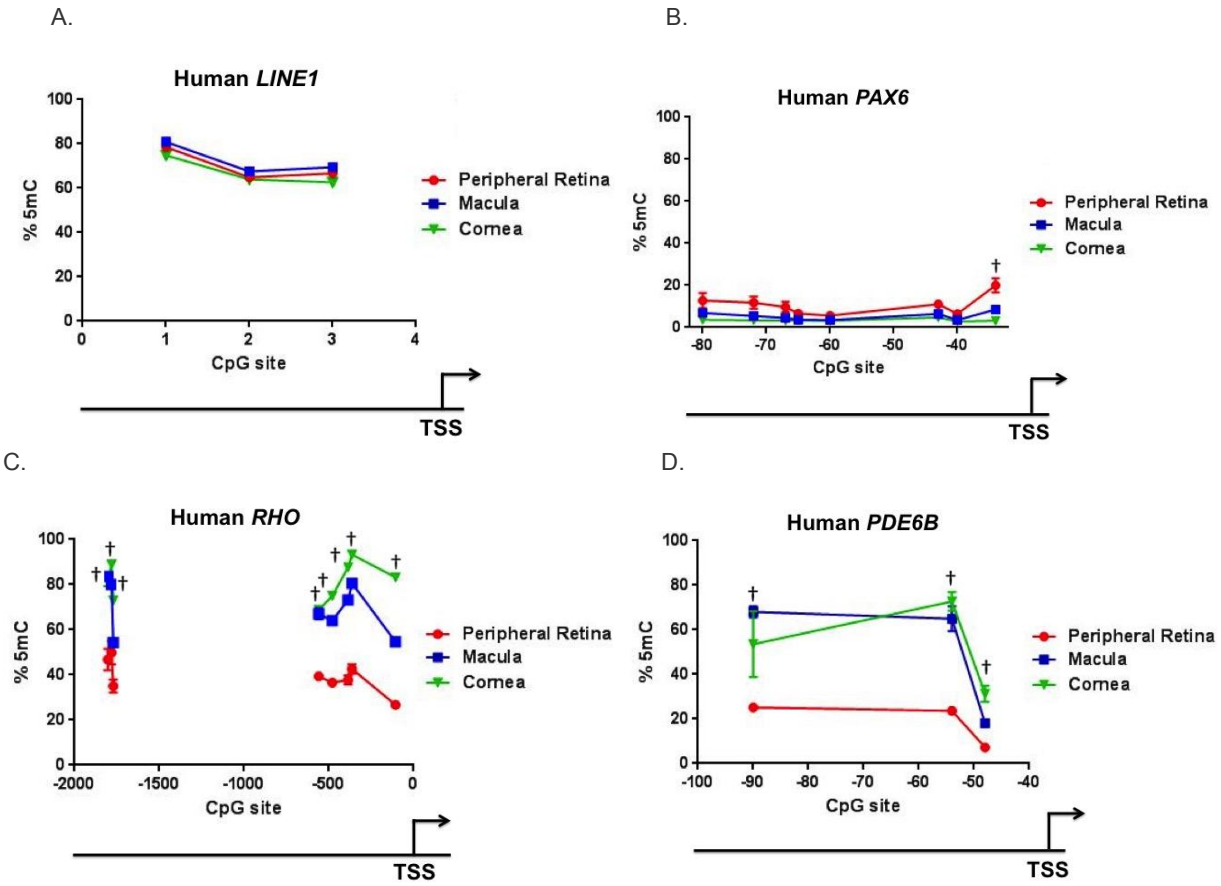

Figure 6. Bisulfite pyrosequencing analysis of Human DNA methylation at CpG sites relative to the transcriptional start site of (A) LINE1 retrotransposon repeats, (B) Paired Box-6, an eye field gene, (C) Rhodopsin, a rod photoreceptor gene, and (D) Phosphodiesterase-6b, another rod-specific photoreceptor gene. Error bars represent standard error of three replicates of cornea samples, and four replicates of peripheral retina and macula samples. Statistical significance of macula and peripheral retina determined by a one-tailed t-test with a $p<0.05$ are denoted by (†).

Expression and Purification of CRX and NRL

The pattern of tissue and cell-specific DNA methylation in predicted CRX binding regions of rod and cone photoreceptor genes of the retina in both mouse and human models prompted further exploration of the biochemical nature of the interaction between DNA methylation and CRX binding. Thus, expression and purification of CRX,

and additionally the NRL protein, was carried out using plasmid constructs designed for affinity purification of the DNA binding domain portions of both proteins (Figure 7).

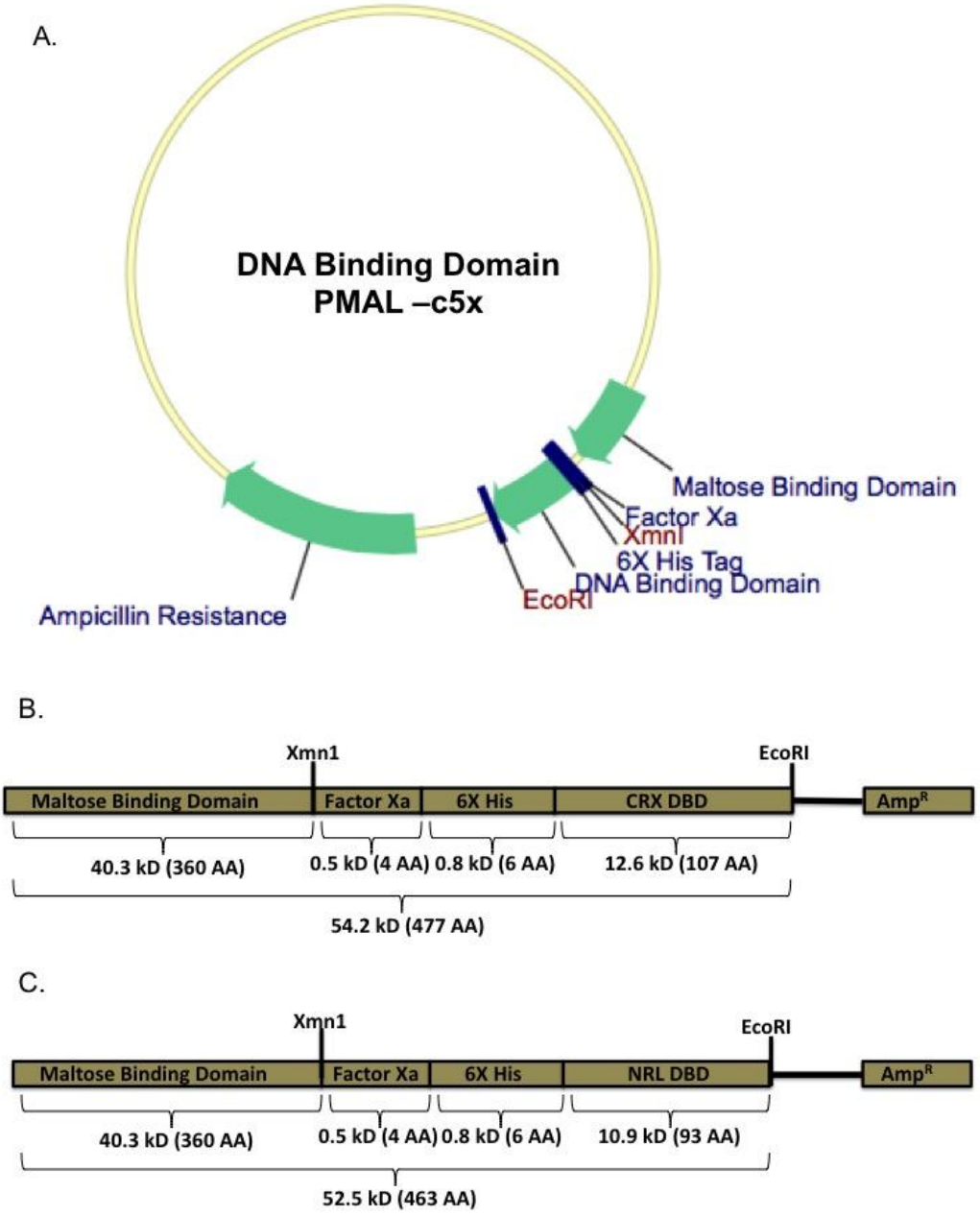

Figure 7. DNA Binding Domain Plasmid Constructs used for Expression. (A) shows the PMAL-c5x vector from GenScript containing the ampicillin resistance gene and maltose binding domain used to clone in the CRX and NRL DNA binding domain sequences. The plasmid maps of the expression constructs of CRX DBD in (B) and NRL DBD in (C) show the predicted sizes of the proteins.

Post-induction time course experiments indicated successful expression of both CRX and NRL DNA binding domain plasmid constructs (Figure 8). The presence of robust bands at approximately 54.2 kDa and 52.5 kDa consistent with the predicted sizes of the CRX and NRL DNA binding domain expressed proteins were observed in the post-induction analysis. The CRX and NRL full length proteins (not pictured) presented problems with expression and purification and were not further characterized in this study.

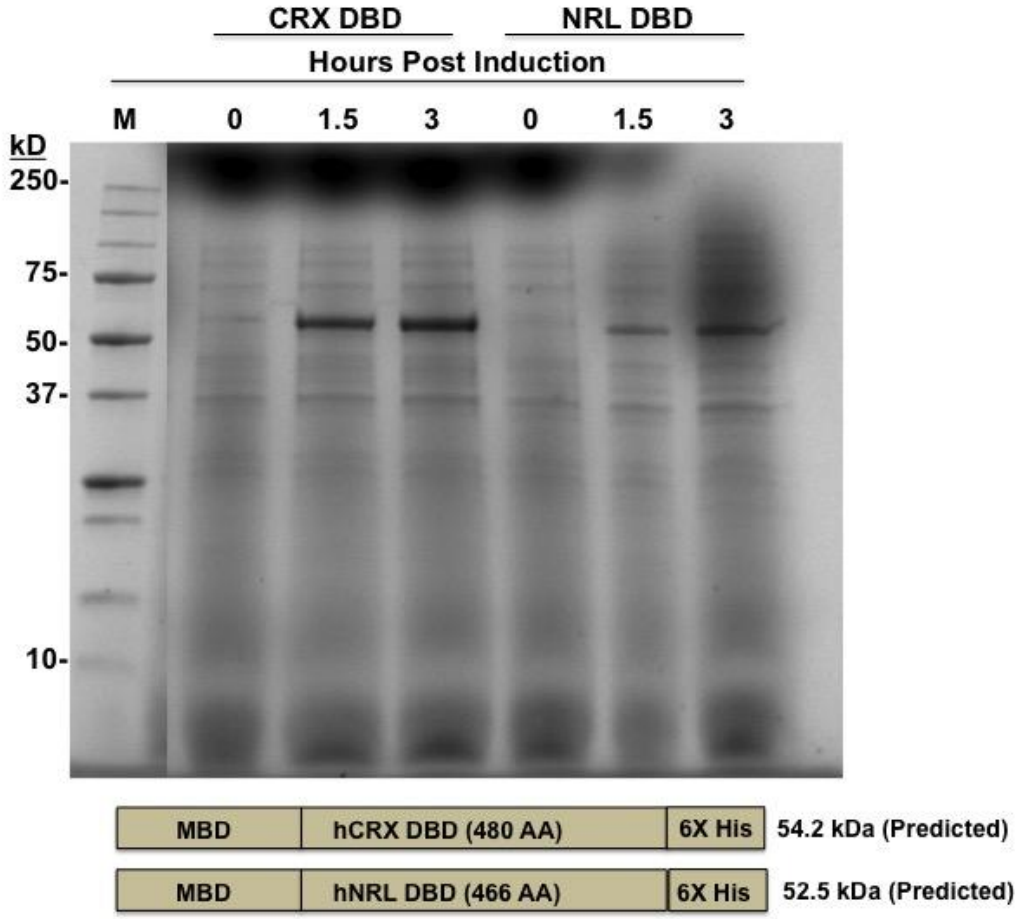

Figure 8. Bacterial expression of CRX and NRL DBD constructs. BL21 *E. coli* cultures harboring CRX DNA binding domain (lanes 2-4) and NRL DNA binding domain protein expression constructs (lanes 5-7) were induced with IPTG and monitored for protein expression at 1.5 hour intervals out to 3 hours post-induction. Protein marker is loaded in lane 1.

Affinity purification of CRX DBD using nickel resin and an increasing gradient of imidazole indicated that the 10 mM imidazole elution contained the CRX DBD (band at approximately 54.2 kDa). The 10 mM Imidazole elution containing CRX DBD was used for binding assay analysis (Figure 9).

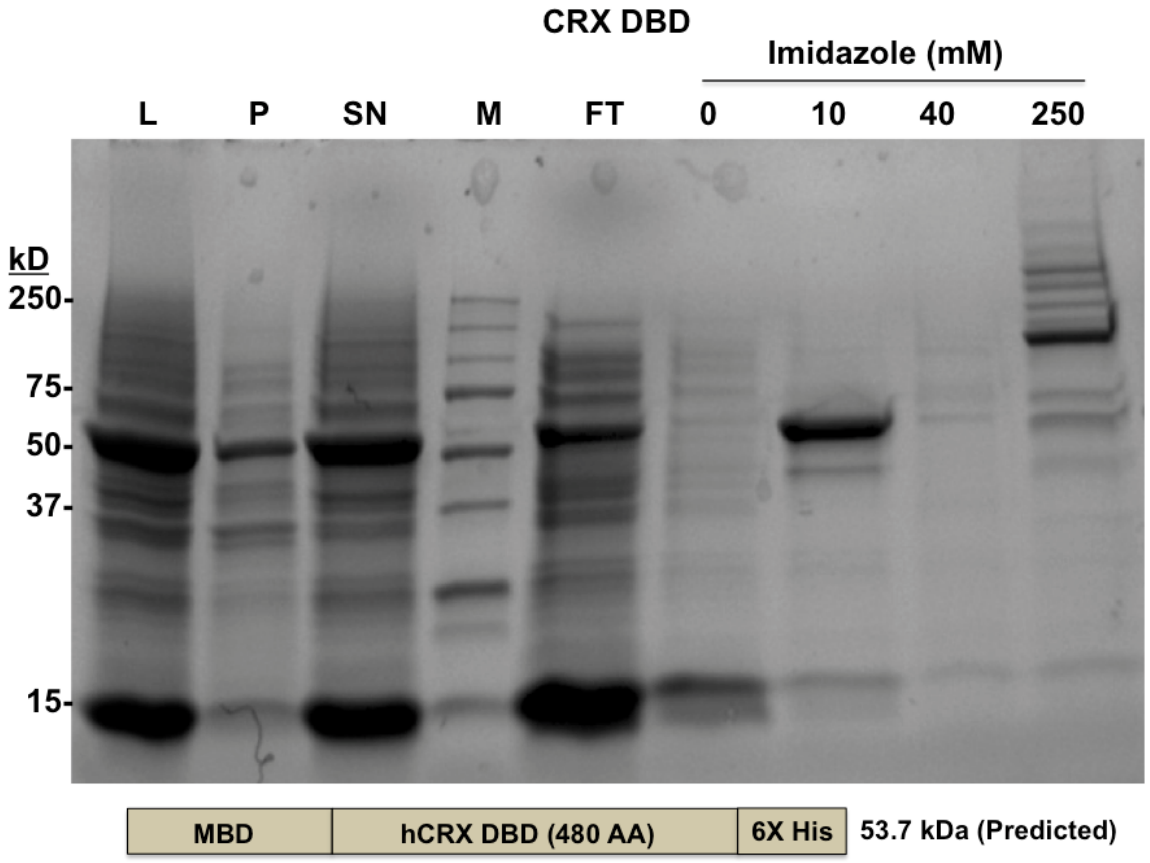

Figure 9. Affinity Purification of CRX DBD using nickel resin. Lane 1 contains the crude lysate after treatment to lyse open the cells prior to centrifugation. Lane 2 contains the pelleted insoluble material and lane 3 contains the supernatant after centrifugation. Lane 5 contains the flow through after placing the prepared supernatant on the column, and lanes 6-9 contain protein elutions after treatment with an increasing gradient of imidazole from 0 mM to 250 mM. Lane 10 contains the left-over beads in the column. The 250 kDa protein marker is loaded into lane 4. The purified protein appears to be present in lane 7 with the 10 mM imidazole elution at approximately 54.2 kDa.

Affinity purification of NRL DBD using nickel resin and an increasing gradient of imidazole indicated that the 40 mM imidazole elution contained NRL DBD (band at approximately 52.5 kDa). The 40 mM imidazole elution containing NRL DBD will be

used for future binding assay analysis characterizing NRL interaction with methylated DNA (Figure 10).

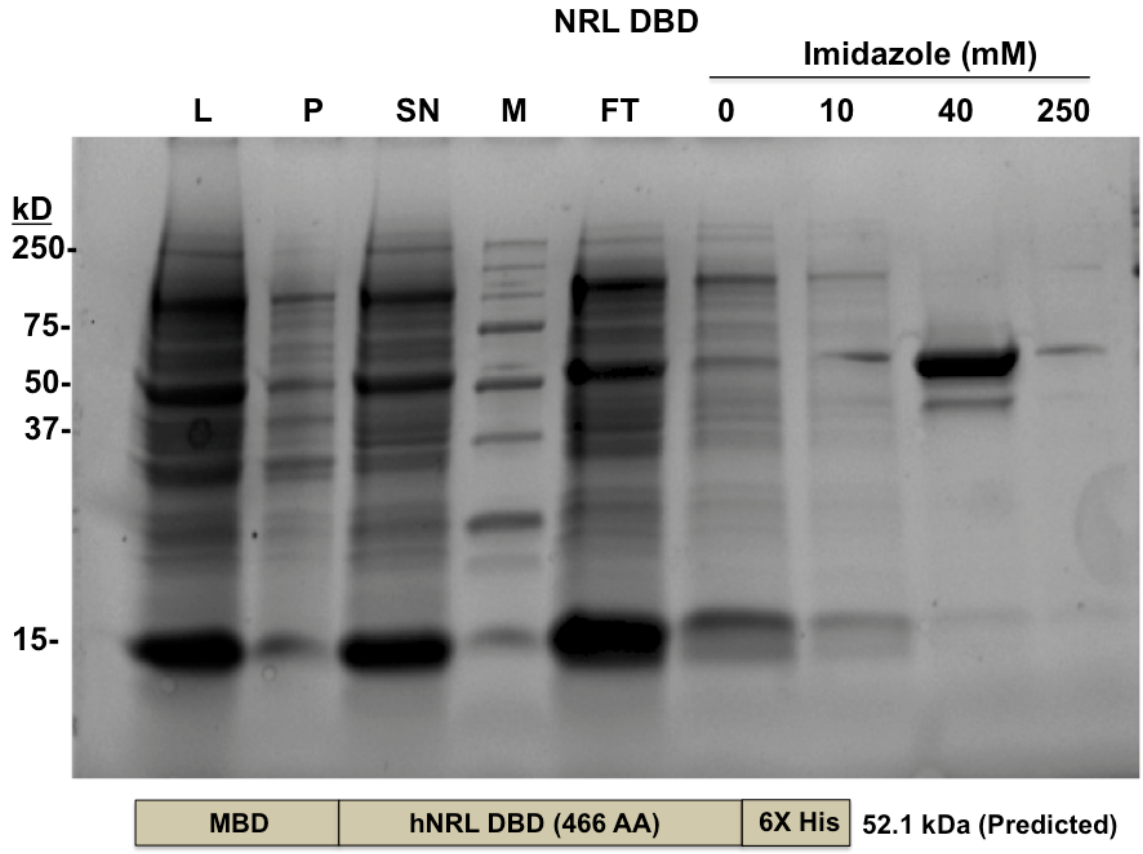

Figure 10. Affinity Purification of NRL DBD using nickel resin. Lane 1 contains the crude lysate after treatment to lyse open the cells prior to centrifugation. Lane 2 contains the pelleted insoluble material and lane 3 contains the supernatant after centrifugation. Lane 5 contains the flow through after placing the prepared supernatant on the column, and lanes 6-9 contain protein elutions after treatment with an increasing gradient of imidazole from 0 mM to 250 mM. Lane 10 contains the leftover beads in the column. The 250 kDa protein marker is loaded into lane 4. The purified protein appears to be present in lane 8 with the 40 mM imidazole elution at approximately 52.5 kDa.

Synthesis of Epigenetically Labeled DNA Probes

Epigenetically labeled DNA probes for use with the purified proteins in electrophoretic mobility shift assays (EMSA) were designed to the upstream enhancer regions of the rod-specific *RHO* gene using bioinformatics analysis in the UCSC

genome browser. In the conserved upstream -5 kb enhancer region of RHO containing a CBR and CRX binding motif, the Cac8I restriction enzyme was chosen as an enzyme sensitive to both DNA methylation and hydroxymethylation (Figure 11B). Digestion of the PCR product with the Cac8I enzyme confirmed that the probe synthesized with each type of dNTP would accordingly mimic conditions to test how methylation and hydroxymethylation affect the ability of CRX and NRL to bind DNA. The -5 kb enhancer probe made with normal dNTPs was cut down to one small band on the gel, while the probes made with 5mCs or 5hCs were entirely blocked from being cut with Cac8I. The 1:1 mix of normal:5mC dNTPs created a probe that was cut into 2 bands by Cac8I, and the same result was observed for the probe synthesized with a 1:1 mix of normal:5hmC dNTPs. No evidence of synthesis was observed in the negative control since dNTPs were not added to the sample (Figure 11A).

In the conserved upstream enhancer region of RHO containing a CBR and CRX binding motif, the HaeII restriction enzyme was chosen as an enzyme sensitive to both DNA methylation and hydroxymethylation (Figure 12B). Digestion of the PCR product with the HaeII enzyme confirmed that the probe synthesized with each type of dNTP would appropriately simulate how methylation and hydroxymethylation affect the ability of CRX and NRL to bind DNA. The enhancer probe made with normal dNTPs was cut down to one small band on the gel. Once again, the probe made with 5mCs was blocked from being cut with HaeII, and the probe made with 5hCs was blocked from cutting as well. Probes made with a 1:1 mix of normal:5mC dNTPs or a 1:1 mix of normal:5hmC dNTPs were cut into 2 bands by HaeII. The negative control showed no evidence of synthesis since no dNTPs were added (Figure 12A).

A.

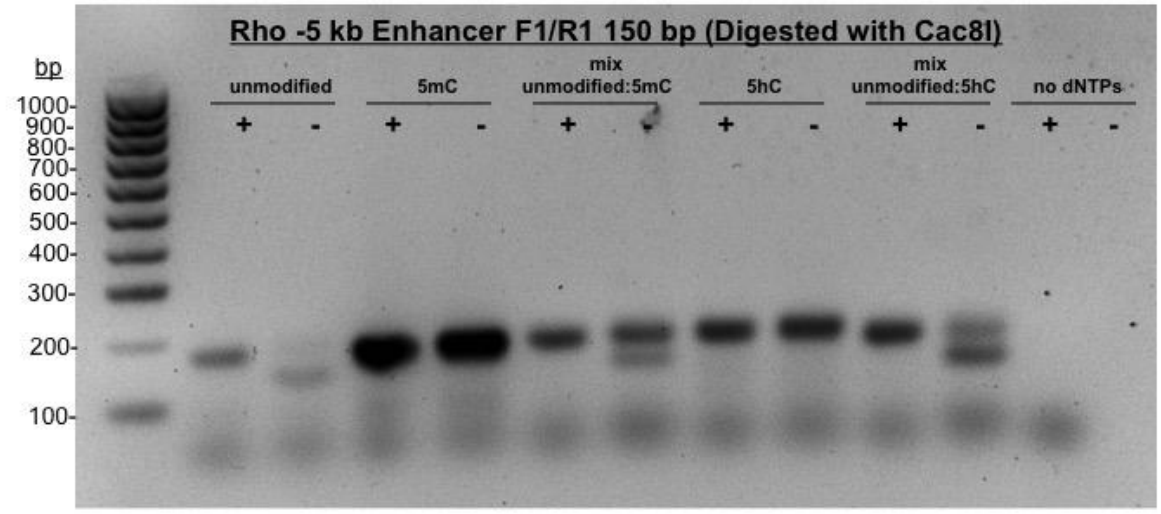

B.

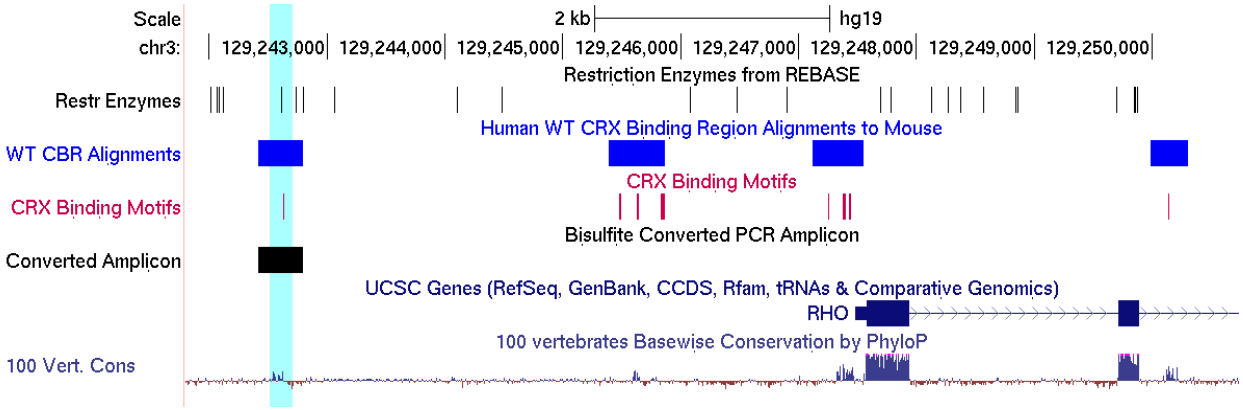

Figure 11. Synthesis of epigenetically labeled DNA probes of the human Rho upstream -5 kb enhancer for EMSA (A) with a genome browser view of the region used to design the probe (B). The epigenetically labeled PCR amplicons were synthesized using normal dNTPs (lanes 2-3), 5mC dNTPs (lanes 4-5), a 1:1 mix of normal:5mC dNTPs (6-7), 5hmC dNTPs (8-9), a 1:1 mix of normal:5hmC dNTPs (10-11), and without any dNTPs as a control (13). The 100 bp ladder is loaded into lane 1. The (+) indicates samples cut with Cac8I and (-) indicates samples that were not digested. The highlighted region of the genome browser (B) shows the upstream enhancer region used to make the probe in which CRX is predicted to bind. The restriction enzymes track shows the Cac8I cut sites used to confirm that CRX may be able to bind the probe when made with certain dNTPs.

A.

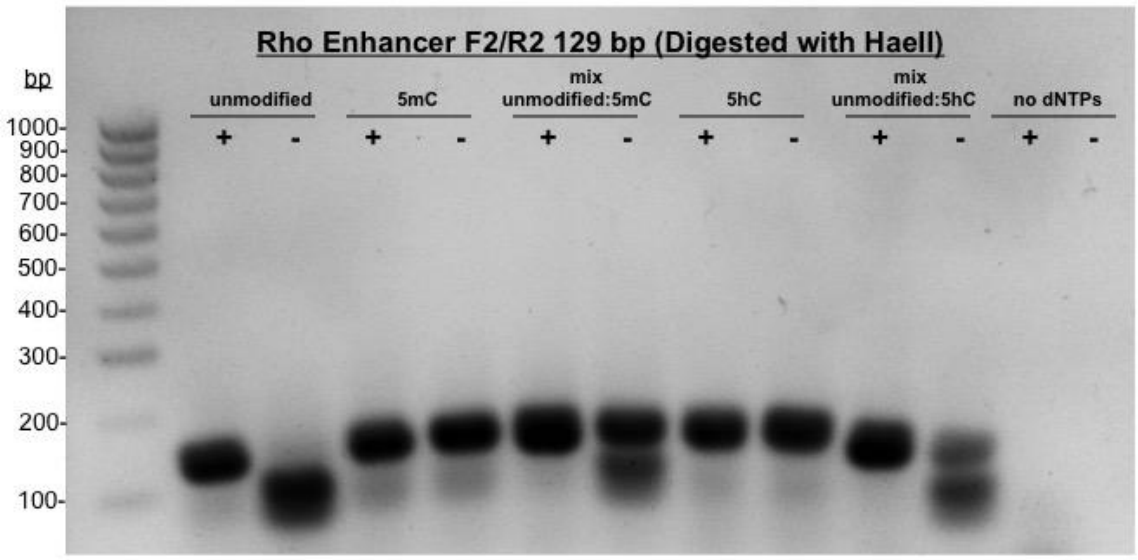

B.

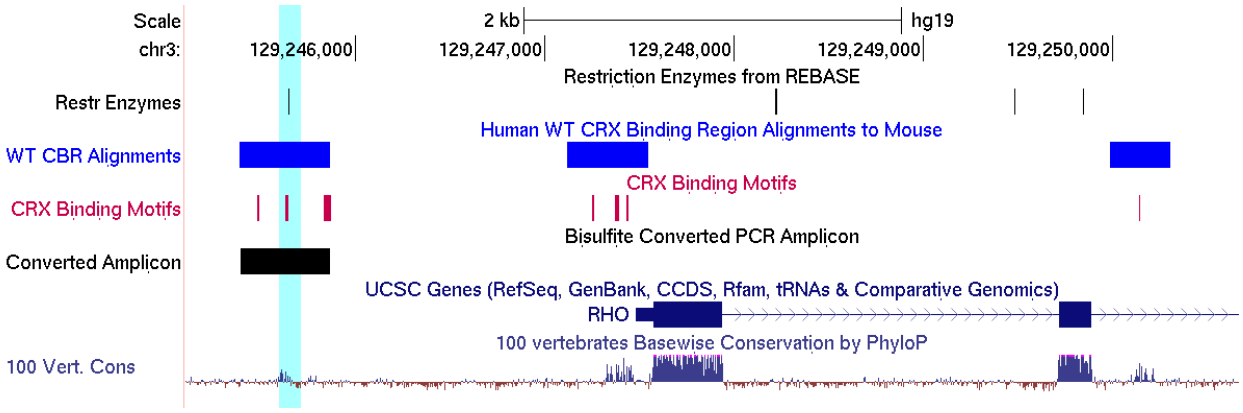

Figure 12. Synthesis of epigenetically labeled DNA probes of the human Rho enhancer for EMSA (A) with a genome browser view of the region used to design the probe (B). The epigenetically labeled PCR amplicons were synthesized using normal dNTPs (lanes 2-3), 5mC dNTPs (lanes 4-5), a 1:1 mix of normal:5mC dNTPs (6-7), 5hmC dNTPs (8-9), a 1:1 mix of normal:5hmC dNTPs (10-11), and without any dNTPs as a control (13). The 100 bp ladder is loaded into lane 1. The (+) indicates samples digested with HaeII and the (-) indicates undigested samples. The highlighted region of the genome browser (B) shows the upstream enhancer region used to make the probe in which CRX is predicted to bind. The restriction enzymes track shows the HaeII cut sites used to confirm that CRX may be able to bind the probe when made with certain dNTPs.

In Vitro Binding Assay

Purified CRX DBD protein was separately incubated with unmodified and epigenetically modified DNA probes containing experimentally validated CBRs.

A.

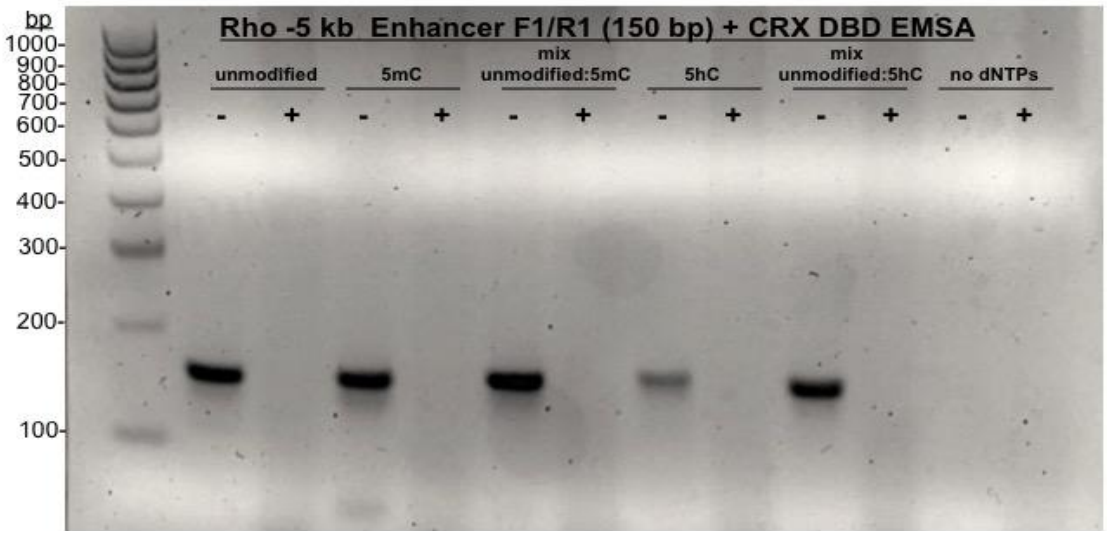

B.

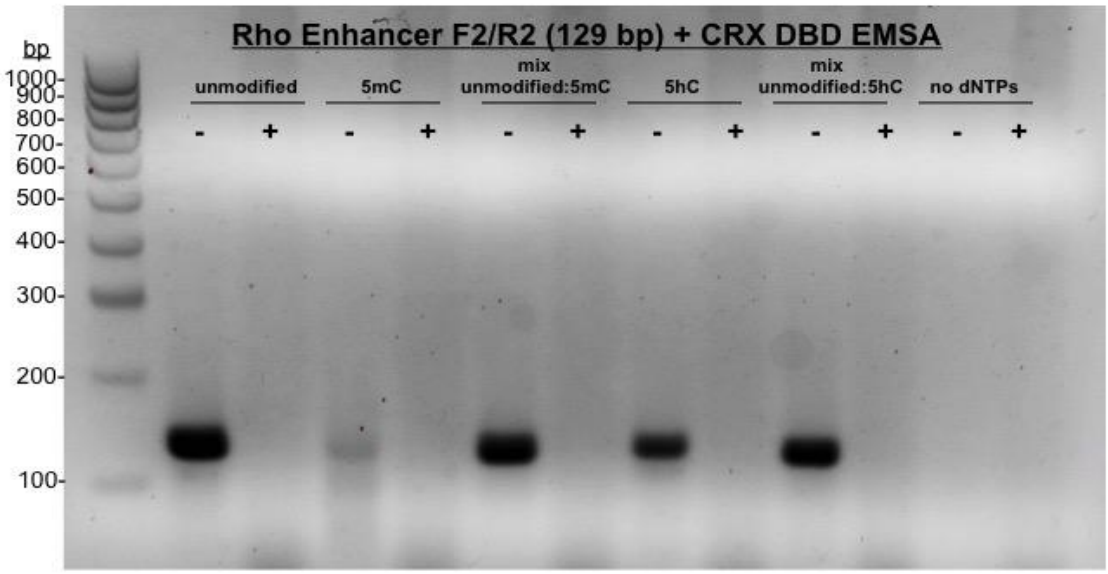

Figure 13. Electrophoretic mobility shift assay (EMSA) showing how methylation and hydroxymethylation affect CRX DBD binding to the upstream -5 kb RHO enhancer (A) and the further downstream enhancer (B). (+) indicates samples mixed with CRX DBD and (-) indicates samples lacking CRX DBD. The epigenetically labeled PCR amplicons were synthesized using normal dNTPs (lanes 2-3), 5mC dNTPs (lanes 4-5), a 1:1 mix of normal:5mC dNTPs (6-7), 5hmC dNTPs (8-9), a 1:1 mix of normal:5hmC dNTPs (10-11), and without any dNTPs as a control (13). The 100 bp ladder is loaded into lane 1.

When protein extract and probes were mixed, no DNA was visible. In control samples in which no protein was added, unshifted probes were visible (data not shown). This result suggested a nuclease activity in our protein purification appeared to cleave the DNA probes . In an effort to ablate this activity, this experiment was repeated in the presence of 50 mM EDTA to chelate metal ions required for nucleases. This modification to the experiment however did not preserve the DNA probes mixed with purified protein (Figure 13). Further modifications to the binding assay procedure are necessary to determine if epigenetically modified DNA has altered interaction with CRX.

DISCUSSION

Through bisulfite pyrosequencing analysis of both human and mouse DNA samples, a tissue and cell-specific pattern of DNA methylation in retina-specific genes was observed. In genes specific to rod photoreceptors (*RHO* and *PDE6B*) within the mouse retina, wt retina had significantly lower methylation compared to wt brain (Figure 4). This relationship between wt retina and wt brain demonstrates a tissue-specific pattern of DNA methylation as rod-photoreceptor genes are less methylated in wt retina tissue rich in rod-photoreceptors. Rod-specific genes would be expected to be highly methylated in the wt brain tissue lacking photoreceptors. This pattern is supported by the inverse correlation between DNA methylation and gene expression (21).

Additionally, the comparison between wt retina and Nrl -/- retina in mice further demonstrated a cell-specific pattern of DNA methylation between photoreceptor cell types inversely correlated with transcription and CRX binding in retina-specific genes. *RHO* and *PDE6B* were significantly less methylated in wt retina than compared to Nrl -/-

retina (Figure 4). The inverse correlation between DNA methylation and transcription supports the observation that rod-specific genes would be less methylated in their cell-specific wt retina tissue and would be highly methylated in a non-cell specific tissue such as Nrl -/- retina rich in cone-photoreceptors.

The tissue and cell-specific pattern of DNA methylation found in regions of the mouse genome presumed to be CRX binding regions of the mouse genome suggests that DNA methylation may regulate the spatial and temporal binding of CRX. To further investigate this observation, the pattern of methylation in Crx - retina suggests a possible explanation for how methylation affects the sequence of events involved in CRX binding and initiating transcription. After CRX binds to its target recognition site, CRX recruits histone acetyltransferases that acetylate local histone tails (25). Chromatin loops then bring the enhancer in close proximity to the promoter and transcriptional start site, and this looping recruits RNA polymerase and initiates transcription (24). The pattern of methylation observed in Crx - retina suggests that unlike the epigenetic modification histone acetylation, CRX is not required for demethylation. In retina in which there is no functional CRX, significantly lower methylation in the rod-photoreceptor specific genes PDE6B and RHO was observed (Figure 4). Thus, it is predicted that because CRX is not required for demethylation, perhaps demethylation of cis-regulatory elements is required for CRX binding to DNA.

Additionally, in close proximity to the regions of the genes analyzed in *RHO* and *PDE6B*, only some CRX binding regions overlap with NRL binding regions (Figure 3). This observation further contributes to the question of what contributes to the spatial and temporal pattern of CRX binding, and if DNA methylation is involved in determining

when and where CRX binds. The pattern of low methylation observed in Crx - retina offers a possible suggestion that demethylation of DNA precedes CRX binding to regulate when and where CRX binds. Collectively, these methylation patterns in mice suggest a possible mechanism of DNA methylation regulating binding of CRX to cis regulatory elements.

Human studies were used to determine if a similar regulatory mechanism exists in primary human retinal tissue. A similar pattern of tissue and cell-specific DNA methylation was also observed in studies of the human retina. Rod-specific genes were observed to have low methylation in the rod-rich peripheral retina, but had significantly more methylation in non-retinal cornea and in macula tissue rich in cone photoreceptors (Figure 6). In these regions of rod-specific genes in which a pattern of tissue and cell-specific DNA methylation was observed, conserved CRX binding regions with CRX motifs were present (Figure 5). Thus, the presence of photoreceptor-specific DNA methylation patterns in regions of the genome where CRX is predicted to bind suggests that DNA methylation is involved in the mechanism of determining when and where CRX binds in human retinal tissue.

To examine the biochemical relationship between DNA methylation and the binding of retina-specific transcription factors CRX and NRL, in vitro binding assays using the DNA binding domain portion of CRX and NRL were attempted. Post-induction analysis indicated successful expression of the DNA binding domains of CRX and NRL. The CRX and NRL full length proteins presented problems with expression and purification. The NRL full length protein was unable to be expressed in BL21 DE3 *E. coli* competent cells, and perhaps transforming the NRL full length construct into a different

strain of cells in the future will allow for successful expression. The CRX full length proteins were successfully expressed; however, attempts to purify the CRX full length protein were not successful. Optimization of expression and purification of these proteins is currently being conducted in the lab. The DNA binding domain proteins became the focus for this study since they proved to be more of a success in expression and purification, and could subsequently be used for in vitro binding assays.

Affinity purification of the DBD proteins using the affinity of the 6X His tag for nickel resin was successful but did not achieve absolute purity of either protein. In both cases of CRX DBD and NRL DBD, the most pure elution with imidazole still left behind several faint bands of contaminating protein. Subsequent purification with ion exchange chromatography as well as concentration of the protein was attempted but did not seem to achieve better purity of the protein (data not shown). Thus, binding assays were attempted using the purified proteins eluted directly from affinity purification with the hope that the proteins would be pure enough despite the lack of total purity.

Analysis of the epigenetically labeled probes in the enhancer regions of the *RHO* gene indicated successful synthesis of methylated and hydroxymethylated probes using various types of dNTP mixtures. Probes made with the two primer sets for enhancer regions of the *RHO* gene known to bind both CRX and NRL showed predicted patterns of digestion with methyl-sensitive and hydroxymethyl-sensitive restriction enzymes.

Binding assays carried out with the F1/R1 probe and the F2/R2 probe incubated with the CRX DBD purified protein appeared to be cleaved by the added protein and were unable to be observed on the gel even in the presence of high molarity EDTA, a metal ion chelator (Figure 13). Thus, it is suspected that the purified protein used for

binding assays most likely possesses residual nuclease activity interfering with binding assays because perhaps the EDTA did not chelate away all of the metal ions. Further modifications to the protein purification scheme for both CRX and NRL DNA binding domain proteins will be used in the future to reduce nuclease activity.

In addition to optimizing the EMSA procedure to see if a detectable change in binding occurs when CRX DBD is added with the epigenetically labeled probes, binding assays with NRL DBD will be carried out. Although NRL DBD was successfully expressed and purified, time did not allow for the protein to be used for binding assays. Additional NRL DBD will need to be expressed and purified for downstream analysis. The CRX full length protein was able to be expressed and purified while the NRL full length protein was not. Expression of the NRL full length protein could be attempted by transforming the construct into a different strain of competent cells other than BL21 DE3 competent *E. coli cells*. After optimizing binding assays with the DBD proteins, it would also be helpful to attempt EMSA with the full length proteins.

Although binding analysis was inconclusive due to procedural setbacks, expression and purification of the CRX and NRL DBD proteins was optimized. Further modifications to the assays will hopefully allow for determination of the sequence of events involved in DNA demethylation and CRX and NRL binding to control expression of retina-specific genes. The tissue and cell-specific patterns of DNA methylation, supported by the inverse correlation between methylation and transcription of both humans and mice suggests that DNA methylation plays a role in determining the spatial and temporal binding of CRX and NRL. Furthermore, the pattern of DNA methylation in observed in Crx - mouse retina suggests that CRX is not required for demethylation,

and perhaps CRX binding is responsible for initiating demethylation of DNA. Collectively, these data suggest a possible role for DNA methylation regulating when and where CRX and NRL bind to cis-regulatory elements to control gene expression in the retina. These data suggest that DNA demethylation of CRX binding sites precedes CRX binding and histone acetylation, which subsequently allows NRL to bind in rod photoreceptors to coordinate expression of photoreceptor-specific genes essential for vision. Optimizing the binding assay procedure will further help to provide support for this hypothesis.

References

1. Kolb, H. “Webvision: The organization of the retina and visual system.” University of Utah, 2017, webvision.med.utah.edu (2017).
2. BrightFocus Foundation. “Facts and Data to Help You Understand Brain and Eye Disease.” BrightFocus, http://www.brightfocus.org, (2017).
3. Francis, P.J. “Genetics of Inherited Retinal Disease.” *Journal of the Royal Society of Medicine* 99.4 (2006): 189–191.
4. Wensel, T.G. "Signal Transducing Membrane Complexes of Photoreceptor Outer Segments." *Vision research* 48.20 (2008): 2052-61.
5. Applebury, M. L. and Hargrave, P.A. "Molecular Biology of the Visual Pigments." *Vision research* 26.12 (1986): 1881-95.
6. Shichida, Y. and Take, M. *Evolution of Opsins and Phototransduction*. The Royal Society, 2009.
7. Bunt-Milam, A., Hurley, J.B., Lerea, C.L.. "Article: A Transducin is Present in Blue-, Green-, and Red-Sensitive Cone Photoreceptors in the Human Retina." *Neuron* 3 (1989): 367-76.
8. Naeem, M.A., Chavali, V.R., Ali, S., Iqba, M., Riazuddin, S., Kahn, S.N., Husain, T., Sieving, P.A., Ayyagari, R., Riazudin, S., Hejtmancik, J.F., Riazuddin, S.A. "GNAT1 Associated with Autosomal Recessive Congenital Stationary Night Blindness." *Investigative ophthalmology & visual science* 53.3 (2012): 1353-61.
9. Hamilton, S. E., and J. B. Hurley. "A Phosphodiesterase Inhibitor Specific to a Subset of Bovine Retinal Cones." *The Journal of Biological Chemistry* 265.19 (1990): 11259-64.

10. Mannu, G.S. "Retinal Phototransduction." *Neurosciences (Riyadh, Saudi Arabia)* 19.4 (2014): 275-80.
11. Chau, K.Y., Chen, S., Zack, D.J., Ono, S.J. "Functional Domains of the Cone-Rod Homeobox (CRX) Transcription Factor." *The Journal Of Biological Chemistry* 275.47 (2000): 37264-70.
12. Ruzycki, P.A., Tran, N.M., Kolesnikov, A.V., Kefalov, V.J., Chen, S. "Graded Gene Expression Changes Determine Phenotype Severity in Mouse Models of *CRX*-Associated Retinopathies." *Genome Biology* 16.1 (2015): 171. *PMC*.
13. Browne, S., Daiger, S., Sullivan, L. "Genes and mapped Loci Causing Retinal Disease." Retinal Information Network, https://sph.uth.edu/retnet/, (2016).
14. Corbo, J.C., Lawrence, K.A., Karlstetter, M., Myers, C.A., Abdelaziz, M., Dirkes, W., Weigelt, K., Seifert, M., Benes, V., Fritsche, L.G., Weber, B.H., Langmann, T. "CRX ChIP-Seq Reveals the Cis-Regulatory Architecture of Mouse Photoreceptors." *Genome Research* 20.11 (2010): 1512-25.
15. White, M.A, Myers, C.A., Corbo, J.C., Cohen, B.A.. "Massively Parallel in Vivo Enhancer Assay Reveals that Highly Local Features Determine the Cis-Regulatory Function of ChIP-Seq Peaks." *Proceedings of the National Academy of Sciences of the United States of America* 110.29 (2013): 11952-7.
16. Mears, A.J., Kondo, M., Swain, P.K., Takada, Y., Bush, R.A., Saunders, T.L., Sieving, P.A., Swaroop, A. "Nrl is Required for Rod Photoreceptor Development." *Nature genetics* 29.4 (2001): 447.
17. Hong H., Douglas S.K., Bernward, K., Johnson, K.R., Cui, K., Gotoh, N., Zang, C., Gregorski, J., Gieser, L., Peng, W., Fann, Y., Seifert, M., Zhao, K., Swaroop,

A. "Transcriptional Regulation of Rod Photoreceptor Homeostasis Revealed by in Vivo NRL Targetome Analysis." *PLoS Genetics* 8.4 (2012): 1-15.

18. Berger, S.L. "The Complex Language of Chromatin Regulation during Transcription." *Nature* 447.7143 (2007): 407-12.
19. Cedar, H. and Bergman, Y.. "Linking DNA Methylation and Histone Modification: Patterns and Paradigms." *Nature Reviews Genetics* 10.5 (2009): 295-304.
20. Bannister, A.J. and Kouzarides, T. "Regulation of Chromatin by Histone Modifications." *Cell Research* 21.3 (2011): 381-95.
21. Dell'Orco, D. and Karl-Wilhelm, K. "Protein and Signaling Networks in Vertebrate Photoreceptor Cells." *Frontiers in Molecular Neuroscience, Vol 8* (2015).
22. Chen, T., He, X., and Zhu, J.K. "Regulation and Function of DNA Methylation in Plants and Animals." *Cell research* 21.3 (2011): 442-65.
23. Merbs, S. L., Khan, M.A., Hackler, L., Oliver, V.F., Wan, J., Qian, J., Zack, D.J.. "Cell-Specific DNA Methylation Patterns of Retina-Specific Genes." *PLoS ONE* 7.3 (2012): 1-9.
24. Jin, B., and Robertson, K.D. "DNA Methyltransferases, DNA Damage Repair, and Cancer." *Advances in Experimental Medicine and Biology* 754 (2013): 3-29.
25. Nasonkin I.O., Merbs S.L., Lazo, K., Oliver, V.F., Brooks, M., Patel, K., Enke, R.A., Nellissery,J., Jamrich, M., Le, Y.Z, Bharti, K., Fariss, R.N., Rachel, R.A., Zack, D.J., Rodriguez-Boulan, E.J., Swaroop, A."Conditional Knockdown of DNA Methyltransferase 1 Reveals a Key Role of Retinal Pigment Epithelium Integrity in Photoreceptor Outer Segment Morphogenesis." *Development (Cambridge, England)* 140.6 (2013): 1330-41.

26. Delatte, B., and François, F. "TET Proteins: On the Frenetic Hunt for New Cytosine Modifications." *Briefings in Functional Genomics* 12.3 (2013): 191-204.
27. Tan, L. and Yujiang G.S. "Tet Family Proteins and 5-Hydroxymethylcytosine in Development and Disease." *Development (Cambridge, England)* 139.11 (2012): 1895-902.
28. Wahlin, K.J., Enke, R.A., Fuller, J.A., Kalesnykas, G., Zack, D.J. "Epigenetics and Cell Death: DNA Hypermethylation in Programmed Retinal Cell Death." *PLoS ONE* 8.11 (2013): 1-13.
29. Santiago, M., Antunes, C., Guedes, M., Sousa, N., marques, C.J. "TET Enzymes and DNA Hydroxymethylation in Neural Development and Function — how Critical are they?" *Genomics* 104.5 (2014): 334-40.
30. Peng, G. and Chen, S. "Crx Activates Opsin Transcription by Recruiting HAT-Containing Co-Activators and Promoting Histone Acetylation." *Human molecular genetics* 16.20 (2007): 2433-52.
31. Peng, G. and Chen, S. *Active Opsin Loci Adopt Intrachromosomal Loops that Depend on the Photoreceptor Transcription Factor Network*. National Academy of Sciences, 2011.